Atmospheric Environment 45 (2011) 4652–4660

Contents lists available at ScienceDirect

Atmospheric Environment

journal homepage: www.elsevier.com/locate/atmosenv

Numerical research of extreme wind-induced dust transport in a semi-arid human-impacted region of Mexico

Luis F. Pineda-Martinez [a,c,*], Noel Carbajal [a], Arturo A. Campos-Ramos [b], Cristina Noyola-Medrano [a], Antonio Aragón-Piña [b]

[a] Instituto Potosino de Investigación Científica y Tecnológica, A. C., Environmental Sciences, Camino a la Presa San José 2055, Col. Lomas 4 sección CP. 78216, San Luis Potosi S.L.P., Mexico
[b] Instituto de Metalurgia, Universidad Autónoma de San Luis Potosí, San Luis Potosí, Mexico
[c] PEIDA, Universidad Autónoma de Zacatecas, Zacatecas, Mexico

ARTICLE INFO

Article history:
Received 4 February 2011
Received in revised form
5 May 2011
Accepted 20 May 2011

Keywords:
Dust storm
PM_{10}
Numerical modeling
Dust characterization

ABSTRACT

A numerical research is carried out to investigate the regional impact of extreme wind-induced dust transport in the central-northern part of Mexico. In boreal winter, strong wind soil erosion processes occur in the arid zones of the Mexican highlands, as a consequence of land use change and land cover change. The effect of land use change and land cover change has consequences in the atmospheric circulation, by altering the balance in solar radiation, albedo, soil moisture and texture, aerodynamic roughness and other surface properties. The anthropogenic impact of land use change from natural vegetation to agriculture lands developed into land degradation and air quality loss by large dust fluxes into the atmosphere. To investigate the magnitude of these erosion processes, we carried out the numerical modeling of a strong dust storm during the passage of a cold front on 18 March 2008. An algorithm based on the friction velocity was implemented for estimating the flux of particulate matter less than 10 μm (PM_{10}) into the atmosphere. It was possible to show how the plume of high concentration of particulate matter propagates through the complex topography of the highland and of the Eastern Sierra Madre to reach large urban zones in the northern part of Mexico and Southern of Texas. In our numerical simulation we estimated roughly that the fraction of PM_{10} emitted during this event was of the order of 9162.72 ton. A direct effect of dust particles is appreciated in the reduction of measured solar radiation.

1. Introduction

Land use change (LUC) and land cover change (LCC) have been identified as having a potential impact on local and global climate. The effects of LUC and LCC on air quality and more generally on global climate change have been documented through changes in the atmospheric circulation by altering the balance in solar radiation, albedo, soil moisture and texture, aerodynamic roughness and other surface properties (Chase et al., 2000). Although, there are other factors affecting the global climate, such as green house gases and growing urban areas (Kalnay and Cai, 2003), some of the effects of LUC on climate are strong dust storms in arid and semi-arid regions. There is a lack of information about the impact of factors linked directly to land surface properties and their relationship with weather and climate at several scales (Chase et al., 2000; Stohlgren et al., 1998). The factor of vegetation cover change affects the regional climate by causing local changes in radiation budgets and surface fluxes modifying the land-atmosphere energy exchange. Furthermore, abrupt discontinuities in land surface properties may lead mesoscale circulations, for instance in urban to rural area transition. In fact, this circulation can be compared to the sea breeze and mountain-valley circulations. It directly affects local atmospheric circulation regimes (Garratt 1993; Sud et al., 1988; Segal et al., 1989).

The most important impact of LUC and LCC in arid zones is linked to soil loss by wind erosion effects. This desertification process is related to recurrent strong wind events in the dry season in semi-arid human-impacted zones (Collado et al., 2002). Furthermore, the dust storm occurrence affects the radiation budget by increasing the air turbidity. Some assessments indicate that the incoming radiation is backscattered to space due to dust

* Corresponding author. Instituto Potosino de Investigación Científica y Tecnológica, A. C., Environmental Sciences, Camino a la Presa San José 2055, Col. Lomas 4 sección CP. 78216, San Luis Potosi S.L.P., Mexico. Tel.: +52 (444) 834 20 00; fax: +52 (444) 834 20 10.
E-mail address: lpineda@ipicyt.edu.mx (L.F. Pineda-Martinez).

1352-2310/$ – see front matter © 2011 Elsevier Ltd. All rights reserved.
doi:10.1016/j.atmosenv.2011.05.056

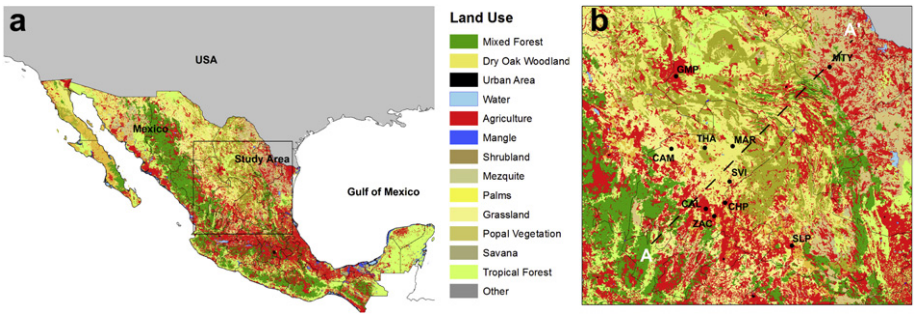

Fig. 1. (a) Land use map of Mexico and location of the study area (box), (b) Applied domain in the numerical simulations. Black dots indicate field weather stations ID's (THA, MAR, SVI, CHP, CAL CAM) and complementary air quality SINAICA stations (ZAC, GMP, MTY, SLP). The transect (A–A′) indicate the position of the vertical cross section in Fig. 6.

particles (Ramanathan et al., 2001; Menon et al., 2002; Loeb and Kato, 2002; Natsagdorj et al., 2003). It has been documented that in summer a direct effect is the reflection of solar radiation due to aerosol produced by biomass burning in tropical forest. However, the dust induced by wind storms in semi-arid regions acquires, in winter, more importance as a contribution to air turbidity in desert and semi-desert regions (Prospero et al., 2002). This kind of dust emission occurs in the northern part of Mexico, but its environmental effect has not been investigated. The soil loss in this region has almost totally an anthropogenic origin by land use change from shrub land and grassland into agriculture, in contrast to the Sahara and other natural desert zones of the world (Prospero et al., 2002; Prospero and Lamb, 2003; Smirnov et al., 2002; In and Park, 2003; Slingo et al., 2006).

The subject discussed in this work is the strong impact of human activities in semi-arid environments. It is evident that under the human pressure, the natural systems have reduced their productivity and they consequently underwent a loss of biodiversity (Reynolds and Stafford Smith, 2002). The reduction or loss of the biological and economic productivity, including soil, vegetation, other biota, and the ecological, biogeochemical, and hydrological processes are partially human induced (Collado et al., 2002). Thus, the main aim of this work is to give insight about land degradation by wind erosion effect. In addition, the impact in a non biotic component, as soil, has consequences in sustainability on food production. Thus, the importance of researching this wind erosion and its relationship with soil loss reside in figuring out desertification process.

The study zone is placed in the highlands in the central north part of Mexico (Fig. 1a). This area has experienced some transformations in land use from mining to rain-fed agriculture, barely irrigated lands and grazing. The decrease of vegetation cover and natural barriers has caused serious problems of soil loss in this highland region of Mexico. In the State of Zacatecas (Fig. 1b), crops and induced grassland increased from 23.72% in 1976 to 32.49% in 2000 (INEGI, 2008). In Fig. 1b, large extensions of agriculture land exposed to wind erosion effect during dry-winter season are shown. The soil loss reaches values of the order of hundreds of tons per hectare in a single strong wind event over the most vulnerable semi-arid agriculture regions (Hagen, 2004; Hupy, 2004). It is important to mention that the soil loss is intensified by wind events, a flat topography and scarce vegetation cover. This erosion process occurs recurrently and dominantly in the dry-winter season, with several events per season and is very variable in terms of the intensity of the winds.

To document dust storms in the Mexican highlands of northern Mexico, a case study in the State of Zacatecas was analyzed. A numerical simulation was carried out for an extreme wind event which caused a severe dust storm. The source of dust was situated in the valley of Guadalupe-Chupaderos, near the city of Zacatecas during March 17 and 18, 2006 (Fig. 1b, see also Fig. 2). The principal land use in the valley is the rain-fed/irrigated agriculture with some patches of secondary grassland and shrublands.

2. Data

The air quality data were obtained from a national network for cities in Mexico, specifically PM_{10} concentrations, (SINAICA, 2008). Additional meteorological data were recorded on automatic meteorological stations as an agroclimatic report on real-time in rural areas (INIFAP, 2008). Rural stations located in the neighborhood of the study area were selected to analyze the behavior of meteorological variables during the passage of the dust storm. Unfortunately, air quality monitoring has only been implemented in the most important urban areas of Mexico; thus, there is a lack of information on the origin and sources under condition of fugitive dust, i.e. dust that is not emitted from definable point sources.

2.1. Dust dispersion modeling

The event was simulated by applying a dispersion numerical modeling of the respiratory particles or particulate matter less

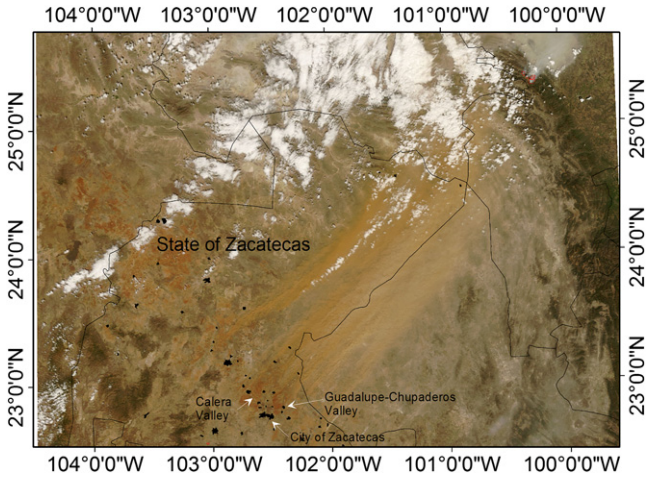

Fig. 2. Moderate Resolution Spectroradiometer image (MODIS) from NASA's Terra satellite. Observe the red-soil land mainly designated to agriculture use that corresponds to source areas of dust. The plumes of dust are appreciated in reddish bands along the wind direction. Also, some wildfires (grayish) appear in the northeast. Low clouds appear in white color. Black dots indicate the main urban areas near the source zones in the State of Zacatecas.

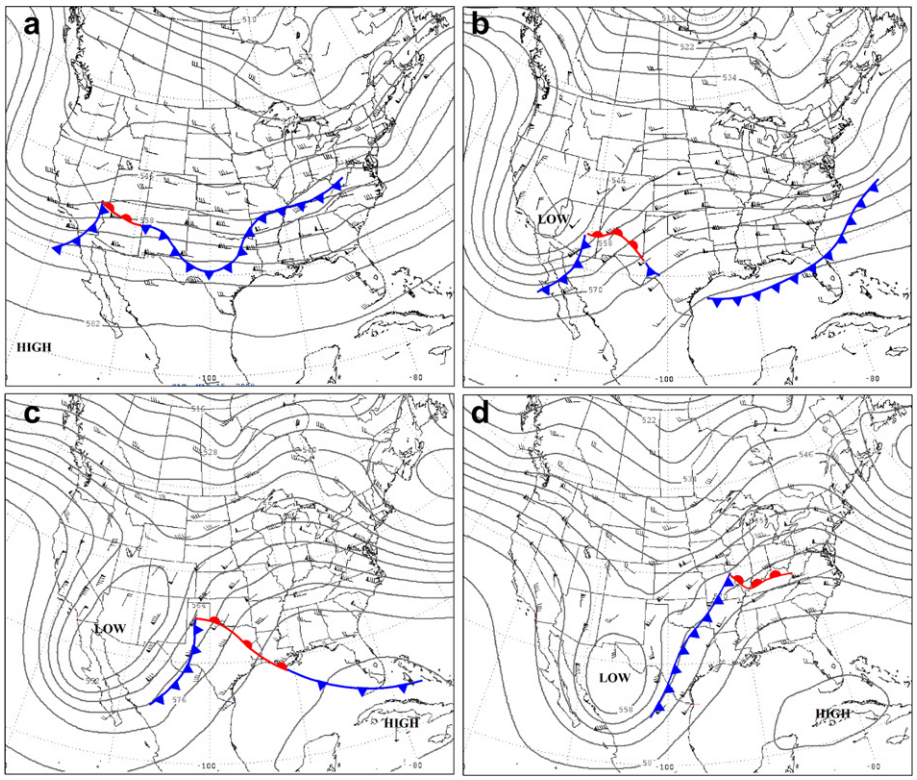

Fig. 3. Upper level charts for 500 hPa height. (a) 00 UT on March 15, (b) 00 UT on March 16, (c) 00 UT on March 17 and (d) 00 UT March 18, 2008 showing geopotential height (black contours) and observed winds. Contour interval 60 m for all charts. Surface frontal positions are indicated (thick black lines). Source: National Centers for Environmental Prediction (NCEP) and Hydrometeorological Prediction Center (HPC).

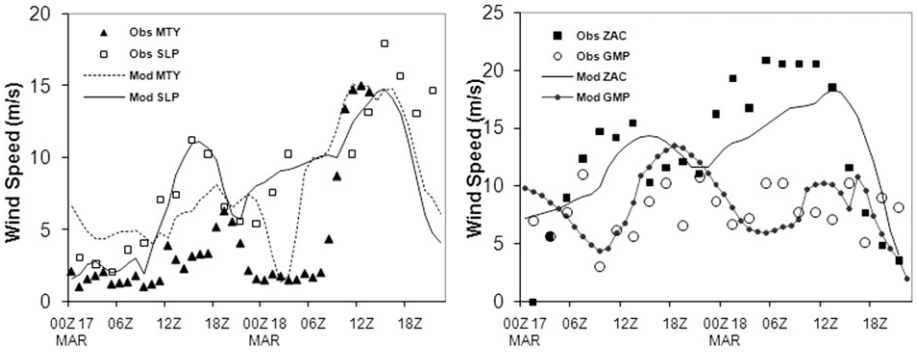

Fig. 4. Wind speed time series of observed and modeled data at four locations (a) Monterrey (MTY) and San Luis Potosi (SLP) and (b) Zacatecas (ZAC) and Torreon (GMP).

than 10 μm (PM_{10}) by applying the Multiscale Climate Chemistry Model (MCCM). The MCCM model is based on the MM5 model (Grell et al., 2000). The MM5 is a non-hydrostatic, three-dimensional and prognostic numerical model (Grell et al., 1994). The sigma (σ) coordinate is considered in the basic equations of the model to determine the vertical levels. It includes multiple nesting capability, non-hydrostatic dynamic and data assimilation in four dimensions. In addition, it offers options for microphysics processes modeling. With the exception of the soil scheme included in the MCCM, the circulation and in general the dynamics are calculated with the MM5 model (Grell et al., 1994). In opposition to non-coupled transport models, the coupling of

Table 1
RMSE and MB values of MCCM outputs and measurements data for meteorological variables.

ID	RMSE			MB		
	T (°C)	RH (%)	V ($m\,s^{-1}$)	T (°C)	RH (%)	V ($m\,s^{-1}$)
ZAC	7.74	37.74	4.70	4.98	−33.49	−0.53
SLP	5.87	20.70	6.92	2.00	−17.45	−0.04
GMP	7.06	20.99	4.35	−0.09	2.34	−1.51
MTY	9.28	29.42	4.69	0.83	−2.55	−3.50
Mean	7.49	27.21	5.16	1.93	−12.79	−1.40

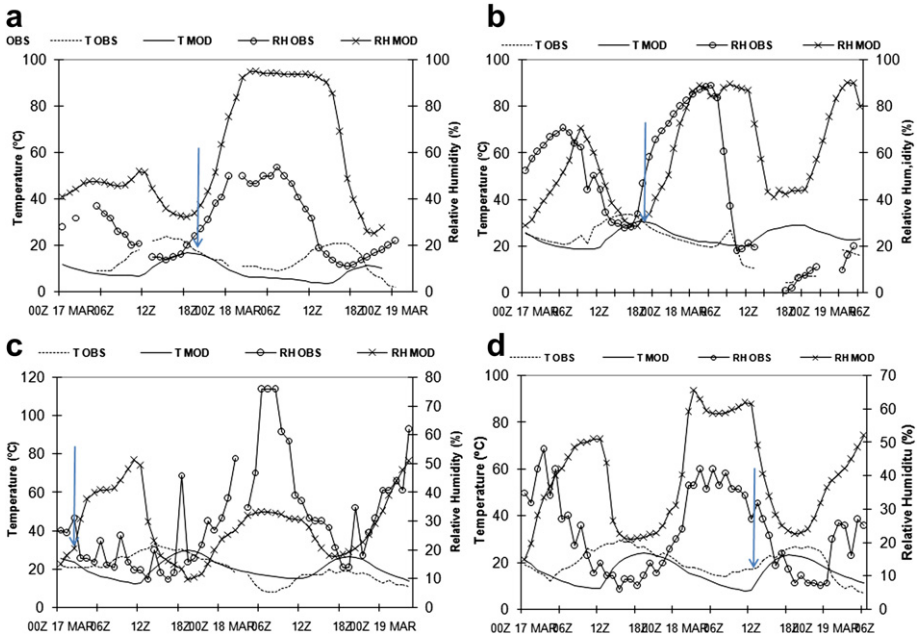

Fig. 5. Time series of observed and modeled data of Temperature (°C) and Relative Humidity (%) at surface level for the period 17–19 March 2008: (a) Zacatecas Station (ZAC), (b) San Luis Potosi (SLP), (c) Torreon Station (GMP) and (d) Monterrey station (MTY). The arrow indicates the arrival time of the front.

meteorology with transport of particulate matter gives consistent results without interpolation of data. The model settings included the parameterization for convection of Grell et al. (1994), the Blackadar boundary layer scheme, the radiation scheme of Dudhia (1989) and the microphysics of warm rain scheme. The model was initiated with the National Centers for Environmental Prediction (NCEP) reanalysis data (Kalnay et al., 1996). This dataset is based on observational and global reanalysis models data with temporal resolution of 6 h and 28 sigma vertical levels. The numerical simulation was initialized at 00Z on 16 March 2008 with duration

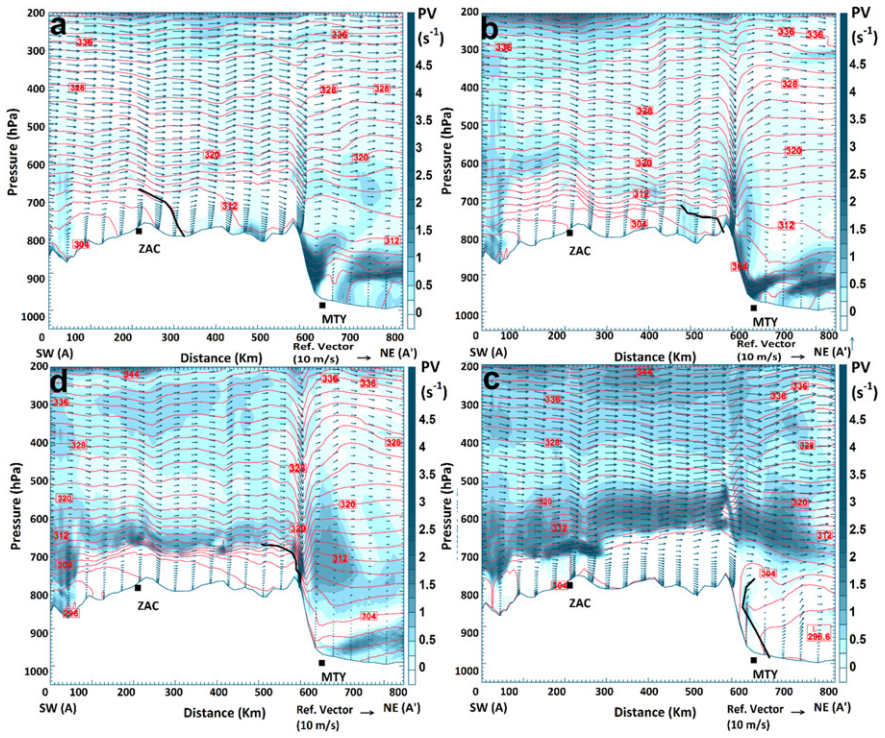

Fig. 6. Vertical cross section SW-NE of wind and temperature for (a) 00 UT, (b) 06 UT (c) 12 UT and (d) 18 UT March 18, 2008. This section extends from the highlands near the city of Zacatecas to Monterrey (see Fig. 1b). Solid red lines represent temperature at 2 K intervals. Shading represents potential vorticity. The arrows indicate wind vectors. The scale for wind vectors is given below. Heavy black lines indicate the position of the surface-based front. This section is oriented in the direction of maximum wind speed. (For interpretation of the references to colour in this figure legend, the reader is referred to the web version of this article.)

96 h with hourly outputs. One single simulation domain D01 was established at central coordinates 24° N and 101.3° W, with a horizontal grid resolution of 12 km on (70 × 70) grid points.

The dust emission flux was determined by applying the proposed vertical mass flux for PM_{10} equation by Choi and Fernando (2008), based in the approach of Westphal et al. (1988). The algorithm consists in a simple estimation of the emitted dust when the friction velocity exceeds the threshold.

$$\mathrm{Fa} = 0.13 \times (1 - R) \times 10^{-14} \times U_*^4 \quad (1)$$

Dust emission occurs when $U_*^4 \geq U_{*t}^4$, where Fa is dust emission flux ($g\,cm^{-2}\,s^{-1}$), R is a vegetation reduction factor, U_* is the friction velocity ($cm\,s^{-1}$), U_{*t} represents the threshold friction velocity. The source areas were limited to bare soil, dry grassland and rain-fed agriculture lands. The friction velocity is estimated using the land surface model of MM5 (Oncley and Dudhia, 1995):

$$U_* = \frac{kU}{\ln\left(\frac{z}{z_0}\right) - \psi_m\left(\frac{z}{L}\right)} \quad (2)$$

where k is the Von Karman constant (0.4), U the wind speed at the height of z, z_0 is the surface roughness length, ψ_m the stability function for the momentum and L the Monin–Obukhov length scale. The threshold friction velocity is determined by comparing field-observed data of wind speed and PM_{10} against modeled U_*. Observed wind speed and PM_{10} at each model grid characterize the dust event when a defined PM_{10} boundary is reached (according to the daily Mexican Official Standard and World Health Organization norm of 150 $\mu g\,m^{-3}$) (NOM, 1993; WHO, 2002).

2.2. Characterization of PM_{10}

In order to obtain specific characteristics of the dust particles, we obtained samples of PM_{10} in the study zone. The obtained data have been used to increase knowledge about the soil properties and the dust emissions in the region. The particles were collected by using a Hi-Vol sampler. The gathering time for each sample was of 24 h, with a constant air flow of 1.3 $m^3\,min^{-1}$ over a period of 72 h. To assess the chemical composition and morphology of individual particles, we applied the methodology described by Aragón et al. (2002). Essentially, this process consists of an analysis applying a Scanning Electron Microscope (SEM). An X-ray diffractometer was employed (DRX) (Rigaku MAX D-2200) to characterize the principal crystalline phases of the collected atmospheric dust.

3. Results

3.1. Description of the dust event

A dust storm initiated in the central part of Mexico on March 17 approximately at 12:00 Local time. The strong winds transported the dust through considerable zones of Mexico reaching the southern part of the State of Texas. The event occurred on 17 and 18 March 2008 during the passage of a cold front, oriented from southwest to northeast, it propagated along the highlands of the northern part of Mexico. Fig. 2 shows the plumes of dust (reddish bands) from the storm and fires (grayish) in the northeast that produces their own plumes of smoke.

The entrance of cold air masses into Mexican highland is very common in winter season. They are associated to intense cold fronts that propagate through the highlands of Mexico (Cavazos and Hastenrath, 1990; Pineda-Martinez and Carbajal, 2009). The mid- and upper-tropospheric front cause intense winds in the leading edge by producing prefrontal pressure trough at the surface as it has been discussed by Schultz (2005). Fig. 3 shows the synoptic conditions that characterized the passage of the frontal event in northwestern Mexico during 15–18 March 2006; the evolution of a low pressure system traveling from Northwest to Southeast is sketched. This pressure trough causes the intensification of surface winds on 17 March approximately at 9:00 Local time, just in the axis along the front.

At the level of 500 mb, the motion of the cold air was governed by the presence of a low pressure (L) region in the southwest of USA and a high pressure (H) region in the central-northwestern part of Mexico, with the whole system moving eastward (Fig. 3c and d). This synoptic situation caused an intensification of winds at the leading edge of the front of the cold air mass (Schultz, 2005). These southwesterly winds were channeled by the topography, reaching gusts of the order of 30 $m\,s^{-1}$. These strong winds originated the removal of soil particles from agricultural areas generating a large dust storm around the city of Zacatecas (22.90°N Lat, −102.52°W Long) (see Fig. 2). The agricultural areas of Calera (CAL), Guadalupe-Chupaderos Valley are characterized by

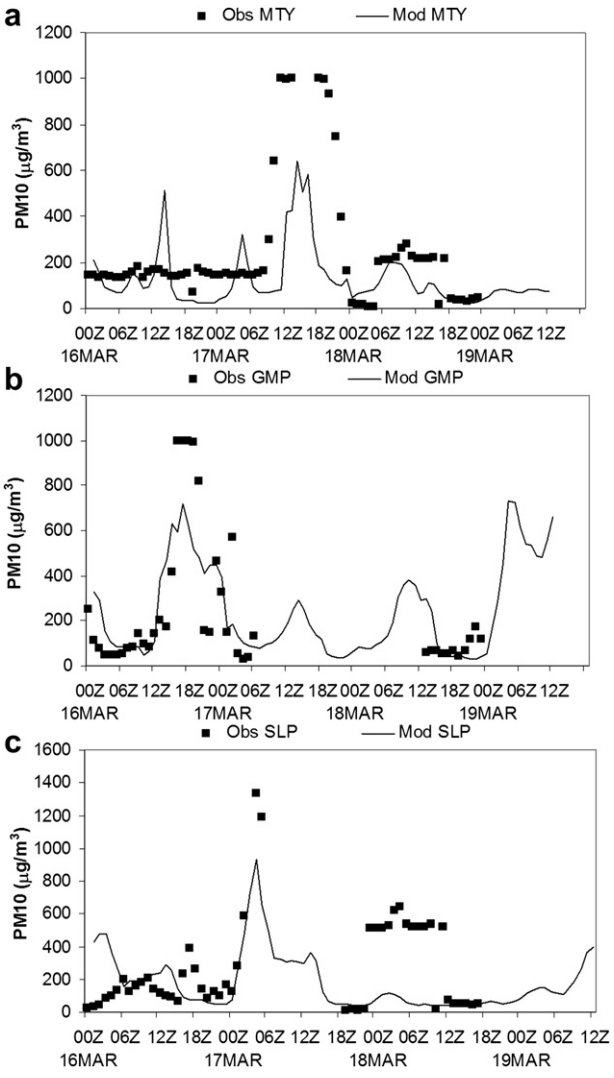

Fig. 7. Modeled and measured PM_{10} concentrations ($\mu g\,m^{-3}$) at three air quality stations (SINAICA) for the period 17–19 March 2008. (a) MTY, (b) GMP and (c) SLP.

a flat topography, 2200 m above the sea level, without the presence of natural topographical barriers. Due to the poor vegetation cover, these regions show a high vulnerability to soil loss in conditions of strong winds ($>10\ m\ s^{-1}$) which are frequent in the dry-winter season (December–March).

3.2. Modeled and measured meteorological variables

The meteorological data were obtained from stations in the surroundings of the source area as well as from stations located on the track of the dust cloud. The wind speed data obtained from the station located in the GP-VC Valley showed two maxima during the event, one of them initiated at 18Z on 17 March 2008 and the other one at 12Z on 18 March. The topographic forcing channeled the leading edge of the cold front causing intense winds in the central part of the highlands (see ZAC in Fig. 1b). In northern regions, for example in City of Monterrey (MTY), the wind was relatively less intense than in ZAC and GMP. Southwards, the event of intense wind was also recorded at the meteorological station in the city of San Luis Potosí (SLP) after a delay of almost 6 h (Fig. 4).

We carried out a model evaluation by calculating the difference between observed and modeled variables. In Table 1 are depicted values for Root Mean Square Error (RMSE) and Mean Bias (MB) of temperature, relative humidity and wind speed. MB reveals that regions under extreme atmospheric circulation conditions, the numerical models have some difficulty capturing the spatial variation and magnitude of the relative humidity and temperature (ZAC and SLP). Although variations in temperature (T °C) and relative humidity (RH %) are modeled for extreme atmospheric conditions such as the cold front passage, the estimated RMSE and MB values are of the same order as those found in other research works (USEPA, 2007; Oncley and Dudhia 1995; Miao et al. 2007; Pineda-Martinez and Carbajal, 2009) (Fig. 5). An additional complication is the presence of mineral dust, since it reflects solar radiation and absorbs environmental moisture by the presence of quartz and silica (Zobeck and Fryrear, 1986). The time series of observed and modeled relative humidity (RH%) indicate that it increases during the passage of the front (Fig. 5). However, this increase is not obvious at Torreon Station (GMP), where the presence of dust and local effects probably modified the relative humidity. The results of the calculations showed that, in general terms, the model captured the principal aspects of the dust storm under extreme weather conditions.

The intensification of the winds was associated to low-level strong winds circulation from the Pacific to the Gulf of Mexico, including the upper level jet circulation. The SW-NE cross sections in Fig. 6 illustrate this motion. The maximum winds are reached in the transition from the highlands to coastal lands near the Gulf of Mexico. The vorticity is displayed in this section to provide evidence of the effect of the gust of winds in the topographic transitions. In some cases the discontinuities in surface properties or elevation gradients induce vertical turbulent fluxes (Chen and Avissar, 1994).

3.3. Dust flux emission and dispersion

The estimated threshold friction velocity was of $60\ cm^{-1}$ for the surface corresponding to rain-fed agriculture, semi-arid grassland and bare soil. All these dust sources embrace 30 Grid points ($4320\ km^2$). The results of the dust emission flux algorithm reveal that the maximum friction velocities were reached in flat topographic regions and consequently the dust flux in bare soil was larger (about $234.45\ kg\ km^{-2}\ h^{-1}$) than in the other regions of the study area. This value is comparable with that reported for other studies in natural deserts (Westphal et al., 1988; Prospero et al., 2002; In and Park, 2003; Slingo et al., 2006). Although, in semi-arid regions the vegetation cover is scarce, some parts of the

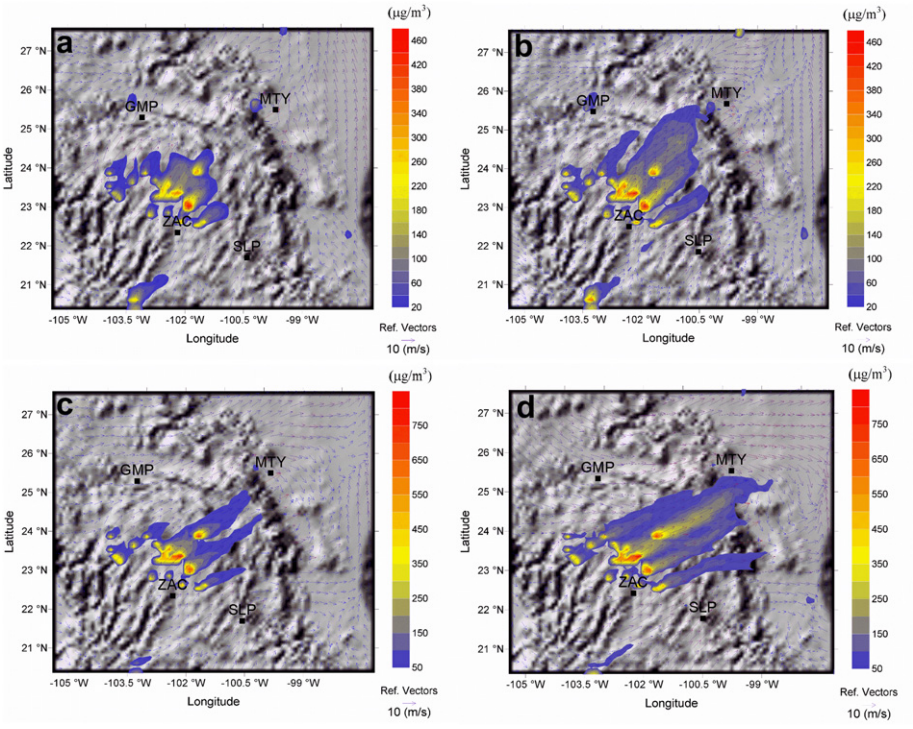

Fig. 8. Numerical results of dust dispersion. Horizontal distribution of PM_{10} (shaded color) and wind vectors on 18 March 2008 at: (a) 09Z, (b) 12Z (c) 15Z and (d) 18Z.

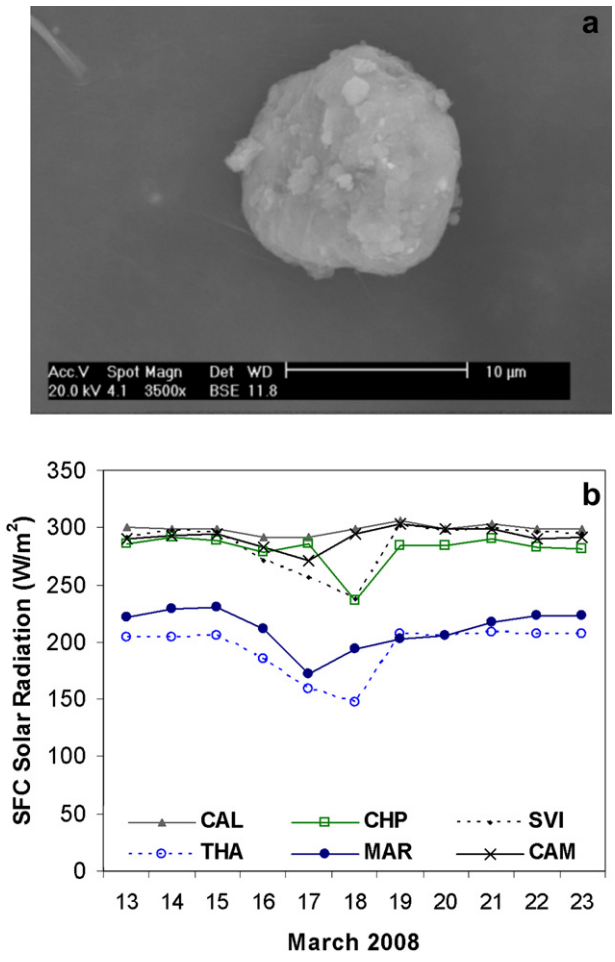

Fig. 9. (a) Photomicrography of the field-collected particle of Microcline ($KAlSi_3O_8$), it is possible to perceive the rounded edges. (b) Surface total radiation (SFC) measured at meteorological stations placed in rural zones in the central-northern part of Mexico: Calera (CAL), Chaparrosa (CHP), Sierra Vieja (SVI), Mazapil 1 (THA), Mazapil 2 (MAR) and Campo Uno (CAM) (Same stations than Fig. 1a) (INIFAP, 2008).

studied region can be considered as a human-induced desert in the dry season (rain-fed agriculture lands). Fig. 7 presents time series of PM_{10} concentrations for three sites. PM_{10} varied mainly by aspects such as transport, dispersion, and deposition processes, vegetation cover and topography. The MM5 and MCCM models reproduce acceptably the principal maxima of the PM_{10} time series. The concentration of PM_{10} particulate matter is clearly above the Mexican Official Standard and World Health Organization norms.

As the cold front propagated southwards, it caused the suspension of dust with several intensities at different sites. Data of concentrations of PM_{10} at City of Torreon station (GMP), located to the northwest of the study area, reveal a maximum value on 17 March 2008 about of 1900UTC. The station located in the city of Monterrey (MTY) registered the arrival of the dust storm in the afternoon of 18 March 2008 increasing the PM_{10} concentration during 3 h. Additional data of PM_{10} concentrations were obtained at the station located in the city of San Luis Potosi (SLP). The highest concentrations of PM_{10} were reached earlier in SLP than in Monterrey (MTY).

Fig. 8 shows a simulation of the passage of the front of the dust cloud through the highlands on 18 March 2008. The circulation and mobility of PM_{10} is well capture by the simulation. The dust emitted was transported from the highlands to northeast across of the Eastern Sierra Madre reaching the southern part of Texas.

3.4. Solar radiation

By SEM analysis of field-collected PM_{10} particles, we distinguish mineral phases of abundant quartz (SiO_2), microcline ($KAlSi_3O_8$) and particles related to anorthite ($CaAl_2Si_2O_8$). These particles are mainly well rounded, with shapes close to spheres (Fig. 9a). The principal morphology of the particles is possibly due to friction processes caused by transport at the land surface. The large quantity of dust transported in the atmosphere modified the incidence of solar radiation, which is reduced by aerosols feedback mechanisms (Ramanathan et al., 2001). In Fig. 9b, a decreased in about 50 $W\,m^{-2}$ for measured solar radiation during the passage of the dust storm is shown. Surface measured solar radiation gives us an idea of the influence of the mineral dust in this human-impacted region. The whole field weather stations recorded a diminution in solar radiation during the passage of the dust. The geographical position of the stations allowed recording the effect of turbidity during the dust passage through the highland. This is the first time that it is documented for dust storms in a human-impacted area in the northern region of Mexico.

The direct effect of dust particles is noted in the reduction of solar radiation. Since the radiation data were measured at stations placed just on the track of the dust storm, it is possible to infer the net reflectivity effect of mineral dust particles (dominantly quartz). The measured solar radiation data showed clearly a minimum during the development of the dust storm. It is important to mention that these stations have no influence from large urban areas. Similar effects have been previously reported for the Sahara and other natural desert zones where emitted mineral dust diminished the solar radiation at the surface level (Prospero et al., 2002; Smirnov et al., 2002; Slingo et al., 2006).

Additionally, numerical experiments showed the differences in downward shortwave radiation under clear and dusty sky (Fig. 10). These results indicate that the presence of suspended mineral material alters the incidence of solar radiation. In Fig. 10, the left side serial of plots shows the model result without considering PM_{10} emission. The right side serial one shows the influence of the presence of the atmospheric dust during its passage through the Mexican highlands. Effects of clouds cover are appreciated in both cases.

Although the maximum wind intensity lasted for a period of 8 h, the threshold friction velocity for dust suspension was reached earlier. It began with moderate levels of concentration, as it was recorded in air monitoring stations, reaching its maximum value in the afternoon and ending this process at about 19:00 h local time. The average dust flux estimated was on the order of 176.75 $kg\,km^{-2}\,h^{-1}$. With this value, a rough estimation of the soil loss for a period of 12 h for a source area of 4320 km^2 was approximately 9162 ton of PM_{10} fraction. These results show the significance of this recurrent problem in the dry-winter season.

The transport of huge quantities of dust shows how relatively small local factors such as land cover change may affect the air quality in large areas and urban zones such as the city of Monterrey, located 400 km from the source area. Further, land cover change generates a local environmental impact through desertification and loss of productivity in cultivated land and affects the weather in the arid Mexican highlands. Finally, an important fraction of the transported particles cumulate in the surroundings of the different valleys initiating dunes formation process, consequently the intensification of land degradation.

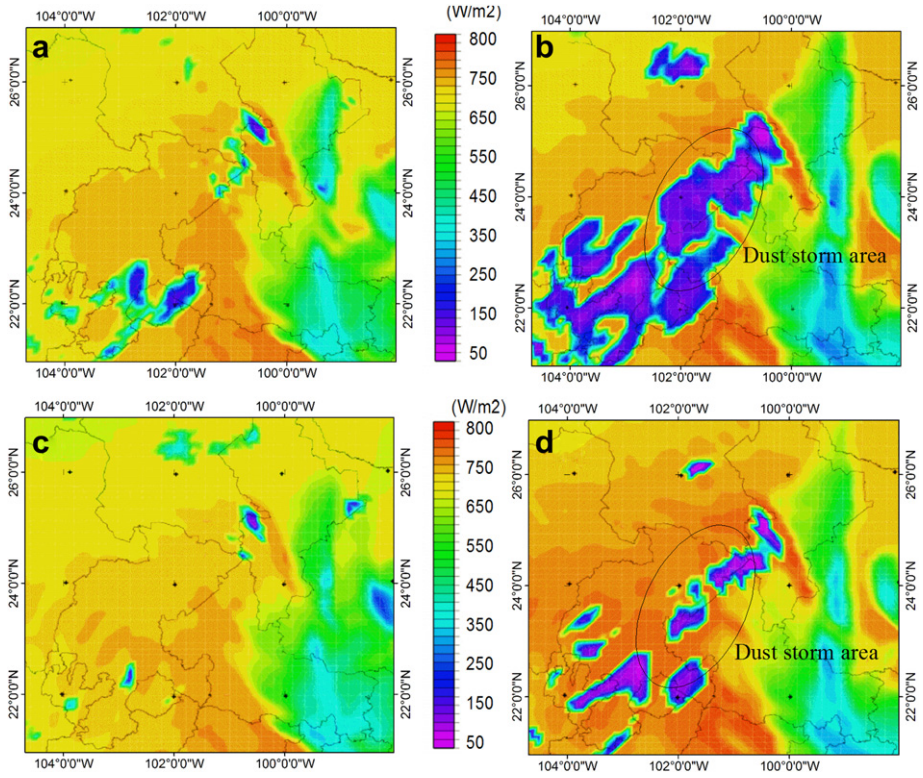

Fig. 10. Distribution of shortwave downward radiation at 15:00 LT and 16:00 LT for two numerical experiments: (a) and (c) MM5 model running without consideration of PM_{10} emissions and (b) and (d) MCCM including PM_{10} particles transported trough Mexican highlands.

4. Conclusions

Numerical modeling has been become in a useful tool to describe complex meteorological phenomena like dust storms in human-impacted areas. The MCCM dispersion model was able to reproduce spatial and temporal characteristics of the event as well as the emissions and concentrations of PM_{10} under a well-modeled atmospheric circulation. The physical and dynamic aspects of a recurrent dust storm in the highlands of the central-northern part of Mexico were presented in a context of land and soil degradation processes. The results showed that a relatively small human-impacted area, by a desertification process, is converted in a source of dust affecting large regions, including urban zones. The analysis of SEM indicated that the morphological characteristics of the collected particles reflect the effects of continuous surface transport in this semi-arid region. The physical properties of the mineral phases of quartz and microcline cause changes in the local weather conditions by reducing the total incident surface solar radiation. The soil management and conservation strategies to mitigate the soil loss must consider policies for agricultural areas by developing programs of rotating crops and considering natural barriers.

Acknowledgments

The authors would like to thank Alfredo Ramos-Leal for his contributions in field journey and comments. We also thank INIFAP Zacatecas for providing radiation field-data of local agriculture monitoring.

References

Aragón, A., Torres, V.G., Santiago, J.P., Monroy, F.M.G., 2002. Scanning and transmission electron microscope of suspended lead rich particles in the air of San Luis Potosi, Mexico. Atmospheric Environment 36, 5235–5243.

Cavazos, T., Hastenrath, S., 1990. Convection and rainfall over Mexico and their modulation by the southern oscillation. International Journal of Climatology 10, 377–386.

Chase, T.N., Pielke, R.A., Kittel, T.G.F., Nemani, R.R., Running, S.W., 2000. Simulated impacts of historical land cover changes on global climate. Climate Dynamics 16, 93–105.

Chen, F., Avissar, R., 1994. Impact of land-surface moisture variability on local shallow convective cumulus and precipitation in large-scale models. Journal of Applied Meteorology 33, 1382–1401.

Choi, Yu-Jin, Fernando, H.J.S., 2008. Implementation of a windblown dust parameterization into MODELS-3/CMAQ: application to episodic PM events in the US/Mexico border. Atmospheric Environment 42, 6039–6046.

Collado, A.D., Chuvieco, E., Camarasa, A., 2002. Satellite remote sensing analysis to monitor desertification processes in the crop-rangeland boundary of Argentina. Journal of Arid Environments 52, 121–133.

Dudhia, J., 1989. Numerical study of convection observed during the winter monsoon experiment using a mesoscale two-dimensional model. Journal of the Atmospheric Sciences 46, 3077–3107.

Garratt, J.R., 1993. Sensitivity of climate simulations to land-surface and atmospheric boundary-layer treatments: a review. Journal of Climate 6, 419–448.

Grell, G.A., Dudhia, J., Stauffer, D.R., 1994. A Description of the Fifth Generation Penn State/NCAR Mesoscale Model (MM5). National Center for Atmospheric Research, TN-398+STR: 138 pp.

Grell, G.A., Emei, S., Stockwell, W.R., Schoenemeyer, T., Forkel, R., Micha-lakes, J., Knoche, J.R., Seild, W., 2000. Application of a multiscale, coupled MM5/chemistry model to the complex terrain of the VOLTAP valley campaign. Atmospheric Environment 34, 1435–1453.

Hagen, L.J., 2004. Evaluation of the wind erosion prediction system (WEPS) erosion submodel on cropland fields. Environmental Modelling & Software Journal 19, 171–176.

Hupy, J.P., 2004. Influence of vegetation cover and crust type on wind-blown sediment in a semiarid climate. Journal of Arid Environments 58, 167–179.

In, H.J., Park, S.U., 2003. Estimation of dust emission amount for a dust storm event occurred in April 1998 in China. Water, Air and Soil Pollution 148, 201–221.

Instituto Nacional de Estadística Geográfica e Informática (INEGI), 2008. Principales tipos de vegetación de México. Sistemas nacionales estadísticos de información geográfica. Available at. http://www.inegi.gob.mx/.

Instituto Nacional de Investigaciones Forestales, Agrícolas y Pecuarias (INIFAP), 2008. Red de monitoreo agroclimático del Eestado de Zacatecas. Available at. http://www.inifapzac.sagarpa.gob.mx/.

Kalnay, E., Cai, M., 2003. Impact of urbanization and land-use change on climate. Nature 423, 528–531.

Kalnay, E., Kanamitsu, M., Kistler, R., Collins, W., Deaven, D., Gandin, L., Iredell, M., Saha, S., White, G., Woollen, J., Zhu, Y., Leetmaa, A., Reynolds, B., Chelliah, M., Ebisuzaki, W., Higgins, W., Janowiak, J., Mo, K., Ropelewski, C., Wang, J.,

Jenne, R., Joseph, D., 1996. The NCEP/NCAR 40-year reanalysis project. Bulletin of the American Meteorological Society 77, 437–471.
Loeb, N.G., Kato, S., 2002. Top-of-atmosphere direct radiative effect of aerosols over the Tropical Oceans from the Clouds and the Earth's Radiant Energy System (CERES) satellite instrument. Journal of Climate 15, 1474–1484.
Menon, S., Hansen, J., Nazarenko, L., Luo, Y., 2002. Climate effects of black carbon aerosols in China and India. Science 297, 2250–2252.
Miao, J.F., Chen, D., Borne, K., 2007. Evaluation and comparison of Noah and Pleim–Xiu land surface models in MM5 using GÖTE2001 data: spatial and temporal variations in near-surface air temperature. Journal of Applied Meteorology and Climatology 46, 1587–1605.
Natsagdorj, L., Jugder, D., Chung, Y.S., 2003. Analysis of dust storms observed in Mongolia during 1937–1999. Atmospheric Environment 37, 1401–1411.
NOM-035-ECOL-1993 Norma Oficial Mexicana, métodos de medición para determinar la concentración de partículas suspendidas totales en el aire ambiente y el procedimiento para la calibración de los equipos de medición.
Oncley, S.P., Dudhia, J., 1995. Evaluation of surface fluxes from MM5 using observations. Monthly Weather Review 123, 3344–3357.
Pineda-Martinez, L.F., Carbajal, N., 2009. Mesoscale numerical modeling of meteorological events in a strong topographic gradient in the northeastern part of Mexico. Climate Dynamics 33 (2–3), 297–312.
Prospero, J.M., Lamb, P.J., 2003. African droughts and dust transport to the Caribbean: climate change implications. Science 302, 1024–1027.
Prospero, J.M., Ginoux, P., Torres, O., Nicholson, S., 2002. Environmental characterization of global sources of atmospheric soil dust derived from the NIMBUS 7 Total Ozone Mapping Spectrometer (TOMS) absorbing aerosol product. Reviews of Geophysics 40 (1), 1–31.
Ramanathan, V., Crutzen, P.J., Kiehl, J.T., Rosenfeld, D., 2001. Aerosols, climate, and the hydrological cycle. Science 294, 2119–2124.
Reynolds, J.F., Stafford Smith, D.M., 2002. Do humans cause deserts? In: Reynolds, J.F., Stafford Smith, D.M. (Eds.), Global Desertification: Do Humans Cause Deserts? Dahlem Workshop Report 88 Dahlem University Press, Berlin, pp. 1–21.
Schultz, D.M., 2005. A review of cold fronts with prefrontal troughs and wind shifts. Monthly Weather Review 133, 2449–2472.
Segal, M., Schreiber, W.E., Kallos, G., Garratt, J.R., Rodi, A., Weaver, J., Pielke, R.A., 1989. The impact of crop areas in northeast Colorado on midsummer mesoscale thermal circulations. Monthly Weather Review 117, 809–825.
Sistema Nacional de Información de la Calidad del Aire (SINAICA v4.0), 2008. Consulta de datos en tiempo real. Instituto Nacional de Ecología (INE). Available at. http://sinaica.ine.gob.mx/.
Slingo, A., Ackerman, T.P., Allan, R.P., Kassianov, E.I., McFarlane, S.A., Robinson, G.J., Barnard, J.C., Miller, M.A., Harries, J.E., Russell, J.E., Dewitte, S., 2006. Observations of the impact of a major Saharan dust storm on the atmospheric radiation balance. Geophysical Research Letters 33, L24817. doi:10.1029/2006GL027869.
Smirnov, A., Holben, B.N., Kaufman, Y.J., Dubovik, O., Eck, T.F., Slutsker, I., Pietras, C., Halthore, R., 2002. Optical properties of atmospheric aerosol in maritime environments. Journal of the Atmospheric Sciences 59, 501–523.
Stohlgren, T.J., Chase, T.N., Pielke, R.A., Kittel, T.G., Baron, J., 1998. Evidence that local and land use practices influence regional climate and vegetation patterns in adjacent natural areas. Global Change Biology 4, 495–504.
Sud, Y.C., Shukla, J., Mintz, Y., 1988. Influence of land surface roughness on atmospheric circulation and precipitation: a sensitivity study with general circulation model. Journal of Applied Meteorology 27, 1036–1054.
USEPA, 2007. Guidance of the Use of Models and Other Analysis for Demonstrating Attainment of Air Quality Goals for Ozone, PM2.5 and Regional Haze. US Environmental Protection Agency, Research Triangle Park, NC.
Westphal, D.L., Toon, O.B., Carlson, T.N., 1988. A case study of mobilization and transport of Saharan dust. Journal of the Atmospheric Sciences 45, 2145–2175.
WHO, 2002. Guidelines for Concentration and Exposure-response Measurement of Fine and Ultra Fine Particulate Matter for Use in Epidemiological Studies. Published on Behalf of the European Commission.
Zobeck, T.M., Fryrear, D.W., 1986. Chemical and physical characteristics of windblown sediment: I. Quantities and physical characteristics. Transactions of the Asabe 29 (4), 1032–1036.